

Fast-Time 2-D Spatial Modulation of Physical Radar Emissions

Patrick McCormick and Shannon D. Blunt

Radar Systems & Remote Sensing Lab (RSL)

University of Kansas

2335 Irving Hill Road Lawrence, KS 66045

email: pmccormick@ittc.ku.edu, sdblunt@ittc.ku.edu

Abstract: *It was recently shown that polyphase-coded frequency modulation (PCFM) waveforms can be expanded to incorporate a spatial modulation coding across a linear antenna array that enables fast-time beamsteering during a transmitted pulsewidth. Here this joint waveform / spatial modulation framework is generalized to two spatial dimensions via a planar array so that complete fast-time spatial steering freedom is available. The resulting emission represents a physically realizable manifestation of MIMO radar that provides enhanced spatial resolution and target discrimination capability using only matched filtering and non-adaptive beamforming. Spatial modulation can also be viewed as a time-varying form of phase-only transmit beamshaping where the significant increase in degrees-of-freedom, relative to static beamshaping, translates into many more possible physically achievable design solutions.*

1. Introduction

In [1,2], linear spatial modulation was introduced as a generalization of the frequency-diverse array concept [3-7] for pulsed emissions. This waveform diversity [8-10] based construct was denoted the waveform-diverse array (WDA) and results from the incorporation of spatial modulation coding into the polyphase-coded FM (PCFM) structure [11,12] that produces physical waveforms amenable for a high-power radar transmitter.

The WDA concept is analogous to the biological operation of fixational eye movement (FEM) in which the eye “wiggles” as a means to improve visual acuity by enhancing contrast and resolving spatial ambiguities [13,14], with a direct linkage to cognitive sensing [15] since FEM adapts to environmental conditions and active attention [16]. Where the WDA structure in [1,2] relied upon a uniform linear array, here this concept is expanded to two spatial dimensions via a planar array which more closely reflects the FEM operation of the eye by permitting freedom of movement in both azimuth and elevation dimensions.

The fast-time spatial modulation of the radar emission represents a specific form of multiple-input multiple-output (MIMO) that, because it leverages the physical PCFM waveform implementation, is likewise a physically-realizable form of MIMO radar. Further, since the WDA structure manifests as a spatially focused beam that moves in fast-time, the RF system issues that can otherwise arise for MIMO radar (i.e. fluctuations in voltage standing wave ratio (VSWR) [17] and distortion due to mutual coupling [18,19]) are avoided.

It is demonstrated by simulation that a notable advantage provided by fast-time spatial modulation is the capability to broaden the mainbeam coverage relative to a focused beam to the extent to which the trade-off in SNR is acceptable. While this broadening could be achieved with beam-spoiling by employing element weightings, the preference for using phase-only weighting limits the degrees of freedom to the number of antenna elements, thus making optimal beam pattern synthesis difficult for modest sized arrays. For this reason, the MIMO approach to beamshaping has received significant attention (e.g. most recently [20,21] and references therein), though the commonly assumed phase coding structure does not meet the requirements for physical emissions [11], nor is the alternative use of simple sinusoids across the elements (e.g. [22]) a practical radar emission strategy. In contrast, spatial modulation provides effective beamshaping while suppressing spatial sidelobes of target returns and modestly enhancing resolution relative to standard beamforming, and possesses a physically-realizable structure that can be readily emitted by a high-power radar.

2. Waveform-Diverse Array (WDA)

The waveform diverse array concept was developed and analyzed in [1,2] for a uniform linear array (ULA). Here the WDA concept is extended for a uniform planar array (UPA) with element spacing d as shown in Fig. 1, for elevation angle θ_z and azimuth angle θ_x relative to antenna boresight.

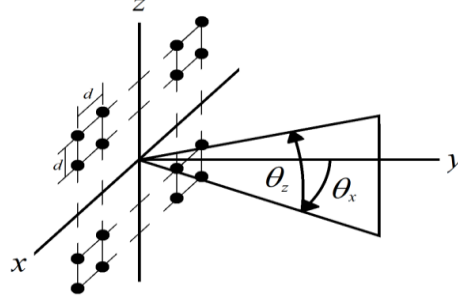


Figure 1. Uniform planar array geometry

The elements of the array in Fig. 1 are indexed as $\mathbf{m} = (m_x, m_z)$ for

$$m_x = -(M_x - 1)/2, -(M_x - 1)/2 + 1, \dots, (M_x - 1)/2 \quad (1)$$

and

$$m_z = -(M_z - 1)/2, -(M_z - 1)/2 + 1, \dots, (M_z - 1)/2, \quad (2)$$

where M_x is the number of horizontal elements and M_z is the number of vertical elements in the UPA. It is assumed the emitted and received signals satisfy the narrowband assumption and thus for the given geometry the wave numbers in the x -dimension and z -dimension, respectively, are [23]

$$k_x = 2\pi d \sin(\theta_x) \cos(\theta_z) / \lambda \quad (3)$$

and

$$k_z = 2\pi d \sin(\theta_z) / \lambda, \quad (4)$$

where λ is the wavelength of the center frequency.

A. WDA Definition

Assuming the capability to generate an independent waveform from each antenna element, the polyphase-coded FM (PCFM) framework [11,12] provides the means to produce a physically-realizable waveform for each element that is controlled by an underlying coding described in [1,2]. Given a polyphase code with $N + 1$ phase values ϕ_0, ϕ_1, \dots , a train of N impulses with time separation T_p are formed such that the total pulsewidth is $T = NT_p$. The n th impulse is weighted by α_n , which is the phase change between successive code values as determined by

$$\alpha_n = \begin{cases} \tilde{\alpha} & \text{if } |\tilde{\alpha}| < \pi \\ \tilde{\alpha} - \text{sgn}(\tilde{\alpha})\pi & \text{otherwise} \end{cases}, \quad (5)$$

where

$$\tilde{\alpha} = \phi_{n-1} - \phi_n \quad \text{for } n=1, \dots, N, \quad (6)$$

and $\text{sgn}(\bullet)$ is the signum operation.

$$s(t; \mathbf{x}_w) = \exp \left\{ j \int_0^t g(\tau) * \left[\sum_{n=1}^N \alpha_n \delta(\tau - (n-1)T_p) \right] d\tau + \phi_0 \right\}, \quad (7)$$

where $*$ denotes convolution, $g(t)$ is the shaping filter, ϕ_0 is the initial phase value of the code, and the sequence of phase changes are collected into the vector $\mathbf{x}_w = [\alpha_1 \ \alpha_2 \ \dots]$ that parameterizes the complex baseband waveform.

In [1,2], the PCFM structure of (7) was extended to include a spatial modulation coding \mathbf{x}_s that is a sequence of spatial phase changes that controls the fast-time steering of the mainbeam in azimuth θ_x . Here the framework is generalized to incorporate spatial modulation in elevation angle θ_z as well. To do so, define the length $N + 1$ sequence of azimuth spatial offsets $\Delta_0^{az}, \Delta_1^{az}, \dots$ relative to some azimuth center direction $\theta_{x,c}$. Likewise, define the sequence of elevation spatial offsets $\Delta_0^{el}, \Delta_1^{el}, \dots$ relative to some elevation center direction $\theta_{z,c}$.

The spatial offset sequences are analogous to the polyphase code ϕ_0, ϕ_1, \dots from which a phase-change code was obtained in (6) to parameterize the continuous waveform in (7). To control the continuous phase functions of the $M_x M_z$ waveforms to provide fast-time beamsteering, azimuth and elevation phase-change codes are also required. Using (3), the azimuth phase-change code is (as a function of code index n) defined as

$$\varepsilon_{x,n} = \frac{2\pi d}{\lambda} \sin(\theta_{x,c} + \Delta_n^{az}) \cos(\theta_{z,c} + \Delta_n^{el}) - \frac{2\pi d}{\lambda} \sin(\theta_{x,c} + \Delta_{n-1}^{az}) \cos(\theta_{z,c} + \Delta_{n-1}^{el}) \text{ for } n=1, \dots \quad (8)$$

Likewise, using (4), the elevation phase change code is

$$\varepsilon_{z,n} = \frac{2\pi d}{\lambda} \left[\sin(\theta_{z,c} + \Delta_{n-1}^{el}) - \sin(\theta_{z,c} + \Delta_n^{el}) \right] \text{ for } n=1, \dots \quad (9)$$

Based on (8) and (9), the azimuth and elevation phase modulations are, respectively,

$$b_x(t; \mathbf{x}_{x,s}) = \exp \left\{ -j \left(\int_0^t g(\tau) * \left[\sum_{n=1}^N \varepsilon_{x,n} \delta(\tau - (n-1)T_p) \right] d\tau + \bar{\Delta}_{x,0} \right) \right\} \quad (10)$$

and

$$b_z(t; \mathbf{x}_{z,s}) = \exp \left\{ -j \left(\int_0^t g(\tau) * \left[\sum_{n=1}^N \varepsilon_{z,n} \delta(\tau - (n-1)T_p) \right] d\tau + \bar{\Delta}_{z,0} \right) \right\}, \quad (11)$$

for $\mathbf{x}_{x,s} = [\varepsilon_{x,1} \ \varepsilon_{x,2} \ \dots]$ and $\mathbf{x}_{z,s} = [\varepsilon_{z,1} \ \varepsilon_{z,2} \ \dots]$ the associated spatial phase-change codes and with initial electrical angles

$$\bar{\Delta}_{x,0} = \frac{2\pi d}{\lambda} \sin(\theta_{x,c} + \Delta_0^{az}) \cos(\theta_{z,c} + \Delta_0^{el}) \quad (12)$$

and

$$\bar{\Delta}_{z,0} = \frac{2\pi d}{\lambda} \sin(\theta_{z,c} + \Delta_0^{el}). \quad (13)$$

The signal generated by the antenna element with the position index $\mathbf{m} = (m_x, m_z)$ is thus

$$s_{\mathbf{m}}(t, \theta_{x,c}, \theta_{z,c}; \mathbf{x}_w, \mathbf{x}_{x,s}, \mathbf{x}_{z,s}) = \frac{1}{\sqrt{T}} s(t; \mathbf{x}_w) \left(b_x(t; \mathbf{x}_{x,s}) \right)^{m_x} \left(b_z(t; \mathbf{x}_{z,s}) \right)^{m_z} \quad (14)$$

where the normalization provides unit transmit energy per antenna element. The incorporation of (7), (10) and (11) into (14) yields the signal generated by the $\mathbf{m} = (m_x, m_z)$ element as

$$s_{\mathbf{m}}(t, \theta_{x,c}, \theta_{z,c}; \mathbf{x}_w, \mathbf{x}_{x,s}, \mathbf{x}_{z,s}) = \frac{1}{\sqrt{T}} \exp \left\{ j \left(\int_0^t g(\tau) * \left[\sum_{n=1}^N \alpha_{n,\mathbf{m}} \delta(\tau - (n-1)T_p) \right] d\tau + \phi_{0,\mathbf{m}} \right) \right\} \quad (15)$$

where $\alpha_{n,\mathbf{m}}$ and $\phi_{0,\mathbf{m}}$ are the composite phase-change sequence and initial phase for element $\mathbf{m} = (m_x, m_z)$ defined as

$$\alpha_{n,\mathbf{m}} = (\alpha_n - m_x \varepsilon_{x,n} - m_z \varepsilon_{z,n}) \quad (16)$$

and

$$\phi_{0,\mathbf{m}} = (\phi_0 - m_x \bar{\Delta}_{x,0} - m_z \bar{\Delta}_{z,0}), \quad (17)$$

respectively. Using (16) and (17), the individual element waveforms can be generated using the CPM implementation described in [1,2].

The normalized baseband representation of the far-field WDA emission for time t and spatial angles θ_x and θ_z can be defined as

$$g(t, \theta_x, \theta_z) = \frac{1}{M_x M_z} \sum_{m_x} \sum_{m_z} s_{\mathbf{m}}(t) e^{j(k_x(\theta_x, \theta_z)m_x + k_z(\theta_z)m_z)} \quad (18)$$

where $s_{\mathbf{m}}(t)$ is from (15) with the terms $\theta_{x,c}$, $\theta_{z,c}$, \mathbf{x}_w , $\mathbf{x}_{x,s}$ and $\mathbf{x}_{z,s}$ suppressed for brevity.

B. WDA Emission Evaluation

To evaluate the impact of 2-D spatially-modulated emission, consider a length $N=100$ waveform code \mathbf{x}_w to closely approximate a linearly frequency modulated (LFM) waveform as described in [12]. The planar array is comprised of 8 elements wide horizontally ($M_x=8$) and 12 elements high vertically ($M_z=12$), with spacing $d=\lambda/2$ and center direction $(\theta_{x,c}, \theta_{z,c})=(0^\circ, 0^\circ)$. The pulse width is normalized to $T=1$ for convenience.

First, Fig. 2a shows the array beampattern when no spatial modulation is present (standard beamforming). In particular, note the narrow beamwidth and the typical lobing structure in azimuth and elevation.

Numerous possible 2-D spatial modulation structures are possible. However, as discussed in [2], there is a trade-off between the diversity enhancement (of spatial resolution and target discrimination) to the SNR loss caused by beam spoiling. Early indications for the linear array case [2] are that little or no further benefit is obtained for the diversity enhancement when the spatial modulation exceeds the first null relative to the center direction. Likewise, the analogy to fixational eye movement supports the notion of relatively small spatial perturbations.

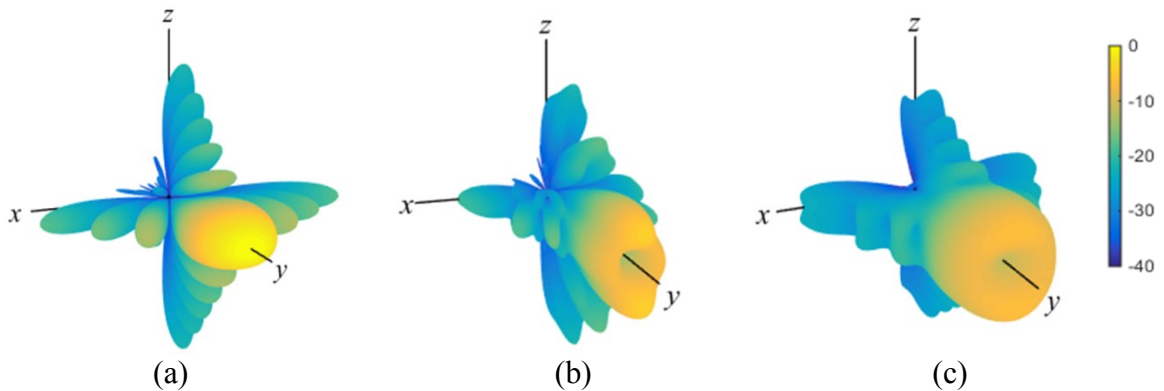


Figure 2. Aggregate beampattern in Cartesian coordinates for (a) standard beamforming; (b) phase-only beamforming; and (c) circular spatial modulation with center direction $(\theta_{x,c}, \theta_{z,c})=(0^\circ, 0^\circ)$

In light of the above justification, consider the simple example of spatial modulation (as defined by the sequences $\mathbf{x}_{x,s}$ and $\mathbf{x}_{z,s}$) in which the emission makes one circular rotation during the pulse around the center direction $(\theta_{x,c}, \theta_{z,c}) = (0^\circ, 0^\circ)$. For the 8×12 planar array, the “radius” of the circular modulation in terms of spatial angle is 9.59° , which corresponds to the first-null in elevation angle.

The aggregate beampattern for this 2-D spatially-modulated emission is shown in Fig. 2b. Notice the partially unfocused nature of the beampattern when spatial modulation is introduced (relative to standard beamforming in Fig. 2a). The movement of the beam during a pulse smears the emitted power in space thus creating blurry response in Fig. 2b. For this case, the loss in peak transmitted power, relative to the fully focused standard beampattern, is 6.4 dB due to the spreading of power in space.

The diversity enhancement that arises from coupling the 2-D spatial dimensions to the range dimension provides a significant reduction in target spatial sidelobes on receive and also improves the ability to discriminate closely spaced targets [1,2].

An alternative method of ‘beam-spoiling’ is imposing a weighting across the array to widen the beam in space. It is advantageous for these weights to have unit-amplitude (phase-only) to maximize transmitted power. Fig. 2c shows an example of phase-only beamforming for 8×12 planar array that has a comparable beampattern to Fig. 2b.

3. Simulation of Physical 2-D MIMO Emissions

The standard beamforming, circular spatially-modulated emission, and phase-only beamforming from the previous section are used to illuminate a simple scenario consisting of two targets in noise to demonstrate the discrimination enhancement provided by spatial modulation and subsequent non-adaptive receive processing of (22) and (23). Both targets occupy the same range cell, with target 1 located at azimuth $\theta_x = 0^\circ$ and elevation $\theta_z = +11.5^\circ$ and target 2 located at azimuth $\theta_x = +1.5^\circ$ and elevation $\theta_z = -3^\circ$.

If a focused transmit beam were directed to each target separately, followed by coherent integration on receive via beamforming and pulse compression, the target SNR values would be 30 dB and 40 dB, respectively. Thus, all emission schemes considered here will exhibit SNR losses for each target. The target locations are chosen such that the spatially-modulated emission and the phase-only beamforming have comparable SNR losses at these locations.

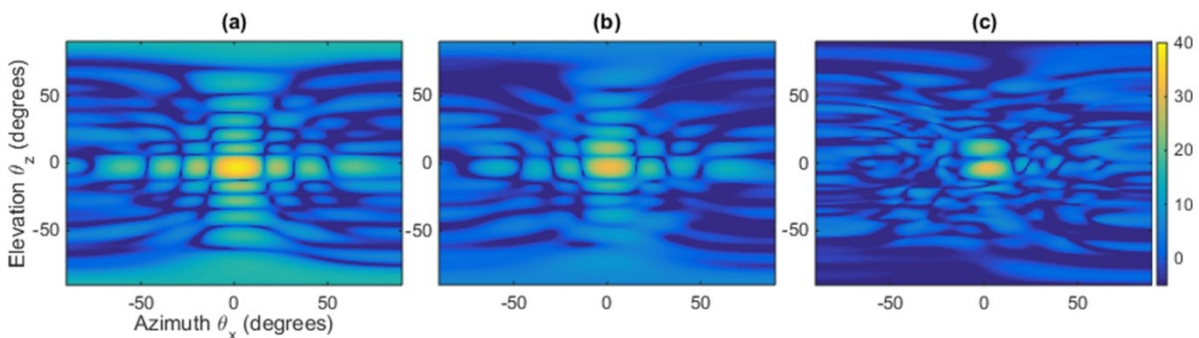


Figure 3. Received response for (a) standard beamforming (b) phase-only beamforming and (c) circular spatial modulation with targets located at $(0^\circ, +11.5^\circ)$ and $(+1.5^\circ, -3^\circ)$

While standard beamforming provides a focused illumination, the spatial separation between the targets prevents the beam from evenly illuminating both targets. As such, only target 2 is visible in Fig. 3a and incurs an SNR penalty of 1.8 dB relative to focused beamforming. In contrast, the phase-only beamforming shown in Fig. 3b does resolve both targets. The SNR losses for targets 1 and 2 respectively are 4.3dB and 8.1 dB. However, spatial sidelobes are still present in both azimuth and elevation and target 1 could easily be

mistaken as the first sidelobe in elevation of the larger target 2. The response using spatial modulation shown in Fig. 3c clearly shows both targets. The SNR losses of targets 1 and 2 are 6.8 dB and 8.5 dB respectively. Spatial modulation has the benefit of suppressing spatial sidelobe of a target, thus alleviating the target/sidelobe ambiguity of the phase-only beamformed case. Each target also has a modest increase in spatial resolution relative to the standard beamforming case. Therefore, the effectiveness of spatial modulation is greatly dependent on the SNR of the illuminated scene but is quite effective for closely spaced targets with sufficiently high SNR.

Conclusions:

A two-dimensional form of fast-time spatial modulation has been developed and demonstrated that represents a form of MIMO that is amenable for use with a high-power radar transmitter (i.e. constant amplitude and well-contained spectrally). This emission scheme provides a modest enhancement to spatial resolution relative to standard beamforming and suppression of target spatial sidelobes while enabling a physically-realizable trade-off between mainbeam coverage and SNR that is reminiscent of the autonomic behavior of fixational eye movement that represents a passive form of cognitive sensing.

References:

- [1] S.D. Blunt, P. McCormick, T. Higgins, M. Rangaswamy, "Spatially-modulated radar waveforms inspired by fixational eye movement," *IEEE Radar Conf.*, May 2014
- [2] S.D. Blunt, P. McCormick, T. Higgins, M. Rangaswamy, "Physical emission of spatially-modulated radar," *IET Radar, Sonar, Nav.*, Dec. 2014.
- [3] Antonik, P., Wicks, M.C., Griffiths, H.D., Baker, C.J., "Range-dependent beamforming using element level waveform diversity," *Intl. Waveform Diversity and Design Conf.*, Jan. 2006.
- [4] Secmen, M., Demir, S., Hizal, A., Eker, T., "Frequency diverse array antenna with periodic time modulated pattern in range and angle," *IEEE Radar Conf.*, Apr. 2007.
- [5] Higgins, T., Blunt, S.D., "Analysis of range-angle coupled beamforming with frequency-diverse chirps," *Intl. Waveform Diversity & Design Conf.*, Feb. 2009.
- [6] Sammartino, P.F., Baker, C.J., Griffiths, H.D., "Frequency diverse MIMO techniques for radar," *IEEE Trans. AES*, Jan. 2013.
- [7] Wang, W.-Q., "Phased-MIMO radar with frequency diversity for range-dependent beamforming," *IEEE Sensors Journal*, Apr. 2013.
- [8] M. Wicks, E. Mokole, S.D. Blunt, V. Amuso, R. Schneible, eds., *Principles of Waveform Diversity & Design*, SciTech Publishing, 2010.
- [9] S. Pillai, K.Y. Li, I. Selesnick, B. Himed, *Waveform Diversity: Theory & Applications*, McGraw-Hill, 2011.
- [10] F. Gini, A. De Maio, L.K. Patton, *Waveform Design and Diversity for Advanced Radar Systems*, IET, 2012.
- [11] S.D. Blunt, M. Cook, J. Jakabosky, J. de Graaf, E. Perrins, "Polyphase-coded FM (PCFM) radar waveforms, part I: implementation," *IEEE Trans. AES*, July 2014.
- [12] S.D. Blunt, J. Jakabosky, M. Cook, J. Stiles, S. Seguin, E.L. Mokole, "Polyphase-coded FM (PCFM) radar waveforms, part I: optimization," *IEEE Trans. AES*, July 2014.
- [13] Rolfs, M., "Microsaccades: small steps on a long way," *Vision Research*, 2009.
- [14] Ahissar, E., Arieli, A., "Seeing via miniature eye movements: a dynamic hypothesis for vision," *Frontiers in Computational Neuroscience*, Nov. 2012.
- [15] Haykin, S., Xue, Y., Setoodeh, P., "Cognitive radar: step toward bridging the gap between neuroscience and engineering," *Proc. IEEE*, Nov. 2012.

- [16] Cui, J., Wilke, M., Logothetis, N.K., Leopold, D.A., Liang, H., "Visibility states modulate microsaccade rate and direction," *Vision Research*, 2009.
- [17] Daum, F., Huang, J., "MIMO radar: snake oil or good idea?" *IEEE AES Mag.*, May 2009.
- [18] B. Cordill, J. Metcalf, S.A. Seguin, D. Chatterjee, S.D. Blunt, "The impact of mutual coupling on MIMO radar emissions," *IEEE Intl. Conf. EM Advanced Applications*, Sept. 2011.
- [19] G. Babur, P.J. Aubry, F. Le Chevalier, "Antenna coupling effects for space-time radar waveforms: analysis and calibration," *IEEE Trans. AP*, May 2014.
- [20] G. Hua, S.S. Abeysekera, "MIMO radar transmit beampattern design with ripple and transition band control," *IEEE Trans. SP*, June 2013.
- [21] S. Ahmed and M.-S. Alouini, "MIMO radar transmit beampattern design without synthesizing the covariance matrix," *IEEE Trans. Signal Processing*, 2014.
- [22] A. Khabbazibasmenj, A. Hassanien, S.A. Vorobyov, M.W. Morency, "Efficient transmit beamspace design for search-free based DOA estimation in MIMO radar," *IEEE Trans. SP*, May 2014.
- [23] Van Trees, H.L., *Optimum Array Processing*, John Wiley & Sons, 2002, Chap. 2.